



ELSEVIER

Available online at www.sciencedirect.com

SCIENCE @ DIRECT®

Nuclear Instruments and Methods in Physics Research B 241 (2005) 436–440

NIM B
Beam Interactions
with Materials & Atoms

www.elsevier.com/locate/nimb

Improvement in the low energy collection efficiency of Si(Li) X-ray detectors

Christopher E. Cox^{a,*}, Daniel A. Fischer^b, Willi G. Schwarz^c, Yongwei Song^a

^a Princeton Gamma-Tech Inc., 1026 Route 518, Princeton, NJ 08553, USA

^b National Institute of Standards and Technology, Gaithersburg, MD 20899, USA

^c Physical Sciences Inc., Sterling, VA 20166, USA

Available online 15 August 2005

Abstract

Soft X-ray beam-line applications are of fundamental importance to material research, and commonly employ high-resolution Si(Li) detectors for energy dispersive spectroscopy. However, the measurement of X-rays below 1 keV is compromised by absorption in the material layers in front of the active crystal and a dead layer at the crystal surface. Various Schottky barrier type contacts were investigated resulting in a 40% reduction of the dead-layer thickness and a factor of two increased sensitivity at carbon K_{α} compared to the standard Si(Li) detector. Si(Li) detectors were tested on the U7A soft X-ray beam-line at the National Synchrotron Light Source and on a scanning electron microscope (SEM).

© 2005 Elsevier B.V. All rights reserved.

PACS: 07.85.Fv

Keywords: Si(Li) detector; Collection efficiency below 1 keV; 14-Channel multi-element array detector; Dead layer

1. Introduction

High-resolution lithium-drifted silicon (Si(Li)) and high-purity germanium (HPGe) detectors are widely used to measure X-rays in the energy range of 1–30 keV in analytical measurement techniques.

A number of studies concerning the response of silicon detectors in the 1–10 keV energy range have been published [1–4]. The detection efficiency is limited at X-ray energies below 1 keV due to absorption by the window in front of the active detector material and an intrinsic dead layer [5] of semiconductor material that can vary with the strength of the electric field at the front contact of the detector. Some calibration work has been published that indicates the Si(Li) detector's efficiency

* Corresponding author. Tel.: +1 609 924 7310; fax: +1 609 924 1729.

E-mail address: ccox@pgt.com (C.E. Cox).

drops very quickly at X-ray energies below 1 keV [3,6]. The development of windowless and ultra-thin windowed Si(Li) detectors has continued since their first use for spectral measurements in the early 1970s [5,7], but until now, little has been published about progress in the fabrication of Si(Li) detector crystals for use in the sub-keV energy range. We have developed a new fabrication process for Si(Li) detectors with significantly improved detection efficiency for soft X-rays below 1 keV.

2. Experiment

Using different, previously untested combinations of surface treatment and metallization, 26 “top hat” geometry Si(Li) detector crystals have been fabricated Fig. 1. Fabrication of the front contact includes chemical etching to remove mechanical damage followed by different wet chemistry processes, evaporation and sputtering of semiconducting or insulating materials under various conditions, such as either a-Ge evaporation, SiO evaporation, Ozone exposure, or no passivation as surface treatment. The subsequent metallization process to form the front electrode has been investigated using different materials and deposition methods. Table 1 summarizes all surface treatment and metallization combinations.

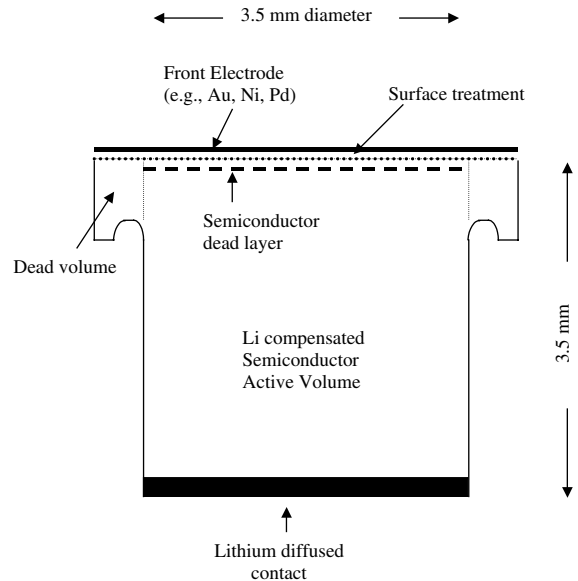


Fig. 1. Experimental X-ray detector cross-section.

It should be noted that the evaporated insulating layers are sufficiently thin (a few Ångströms) to not form an electrically insulating barrier underneath the metal electrode.

The corresponding spectral characteristics were measured and analyzed using either an ^{55}Fe laboratory source or electron beam excitation of a silicon carbide sample. The performance of a prototype 10 mm^2 detector fabricated using process

Table 1
Spectral characteristics measured for tested Si(Li) detector fabrication processes

Process	Surface treatment	Contact metal	TCL (%)	Tail factor (%)	Peak/Bg at 1 keV	Mn FWHM (eV)	C FWHM (eV)	C FWTM/ FWHM	C peak (eV)
Original process	No treatment	150 Å Au/Pd	3.3	0.18	2.0	133	73	1.93	260
X002	50 Å a-Ge	150 Å Au/Pd	2.3	0.11	3.7	136	66	1.94	274
X003	50 Å a-Ge	150 Å Au/Pd	2.0	0.10	3.7	134	62	2.04	276
X004	50 Å a-Ge	150 Å Ni	1.8	0.14	11.7	148	95	1.91	275
X006	50 Å a-Ge	150 Å Au/Pd	2.2	0.13	5.0	132	66	1.91	272
X007	50 Å a-Ge	300 Å Ni	1.8	0.12	3.9	130	62	1.88	269
X008	Ozone exposure	150 Å Au/Pd	3.1	0.17	4.3	128	65	1.85	238
X009	Ozone exposure	300 Å Ni	1.8	0.13	18.3	130	67	1.87	252
X010	No treatment	300 Å Ni	2.0	0.10	5.9	128	158	>2	260
X011	50 Å a-Ge	150 Å Pd	1.7	0.07	4.8	132	72	1.87	270
X013	50 Å SiO	150 Å Au/Pd	1.7	0.07	5.6	129	61	1.86	275
X015	50 Å SiO	300 Å Ni	—	—	—	—	—	—	—

Processes X2, X3 and X6 differ in small changes to the size of the passivated area.

X013 was also tested on the U7A beam-line at the National Synchrotron Light Source (NSLS) at Brookhaven National Laboratory (BNL). The beam-line provides a high intensity, monochromatic photon source that is tunable in the energy range from about 0.1 to 1.1 keV and thus an ideal source for high sensitivity X-ray fluorescence measurements at low energies. In order to increase the detection efficiency while maintaining high energy resolution, a 14-channel multi-element array detector system with multi-channel readout digital signal processors was manufactured using the improved crystal fabrication process. This system was also tested on the NSLS U7A beam-line.

3. Results and discussion

Fig. 2 shows the typical spectrum for detectors fabricated by the original process and the optimized process X013 using an ^{55}Fe source. Table 1 summarizes the main spectral characteristics resulting from the tested Si(Li) detector fabrication process. These parameters include the ^{55}Fe spectrum measurements of Tail Factor [8], Peak-to-Background [9] and Total Charge Loss (TCL) [10]. Whereas the Tail Factor measures the peak asymmetry and the Peak-to-Background measures the height of the plateau region below the peak, the TCL is a measure of the total incomplete charge collection (from all sources) below the main peak. In addition, spectra were collected using an

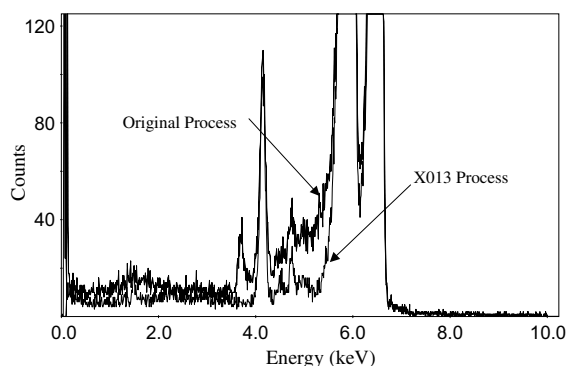


Fig. 2. Comparison of the ^{55}Fe spectra between the original process and the X013 process.

SEM with a Carbon sample to measure the low energy peak shape and linearity. All the measured parameters are affected by charge loss arising from absorption in the window region, for example by carrier diffusion into the dead layer (weak field region) at the front contact [11,12]. The dead-layer results from surface band bending and is dependent on the surface treatment applied and the type of contact metallization used [13–18]. The results show that the Tail Factor is affected mostly by the surface treatment, but the type of metallization correlates with the Peak-to Background ratio. The product yield for Ni metallization was generally low and near zero for process X015. Thus process X013 (SiO passivation + Au/Pd metallization) was deemed to provide the best combination of the measured parameters, offering an improvement by a factor 2 or more in both the TCL and Tail Factor compared to the original process.

Fig. 3 shows the comparison of SiC spectra that have been measured with Si(Li) crystals fabricated using process X013 and the original process, respectively, taken under identical conditions in an SEM. From the improvement in the ratio of the C peak to the Si peak, it can be estimated that the dead-layer thickness has been reduced from about 0.1 μm in the original process to about 0.06 μm in process X013. The position and shape of the Carbon peak are near ideal for the new process crystal compared to the low energy shift and tail of the Carbon peak detected with the old process crystal.

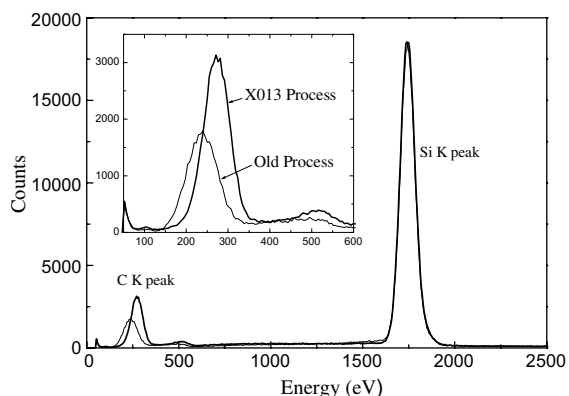


Fig. 3. Energy spectrum of silicon carbide excitation by a 10 keV electron beam in an SEM.

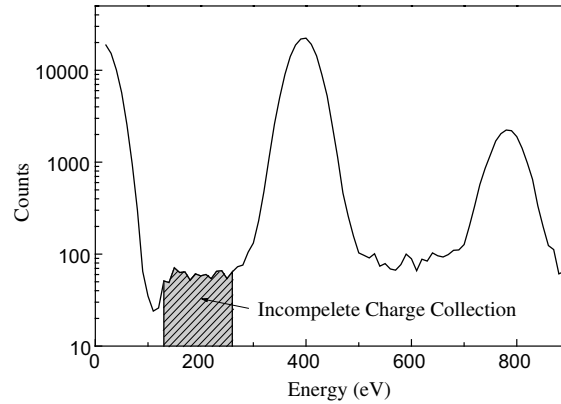


Fig. 4. Energy spectrum at 400 eV incident beam from the X013 process detector tested at NSLS beam-line U7A.

Measurements were performed on the U7A beam-line at the NSLS at Brookhaven National Laboratory with the goal of measuring the detection efficiency as a function of photon beam energy directly incident on the detector face (highly attenuated) and to determine the correlation of dead-layer thickness with spectral characteristics. Fig. 4 shows the spectrum at 400 eV beam energy, which clearly demonstrates the flat incomplete charge collection plateau in the energy range between about 140 and 260 eV. The edge below 140 eV indicates the count roll-off due to the programmed digitization threshold. The peak at 400 eV is the signal from the primary photon beam, and the peak at 800 eV is the signal from beam harmonics. Preliminary analysis of the data for all measured photon beam energies confirms the general trend of the Peak-to-Background versus energy dependence. A 14-element detector utilizing a 2-D array of Si(Li) crystals fabricated with the new process was also designed and installed on the U7A beam-line. This system provides 14 times larger active area (or efficiency) than a single element detector but the resolution is the same. The multi-element system was first tested with an ^{55}Fe source and provided 140 mm² active collection area with energy resolution better than 133 eV at 5.9 keV. Fig. 5 shows a spectrum from the multi-element detector (all channels summed together) with a Boron Nitride sample excited by a 200 eV synchrotron X-ray beam. The excellent low energy collection efficiency, energy resolution and peak shape are self-evident.

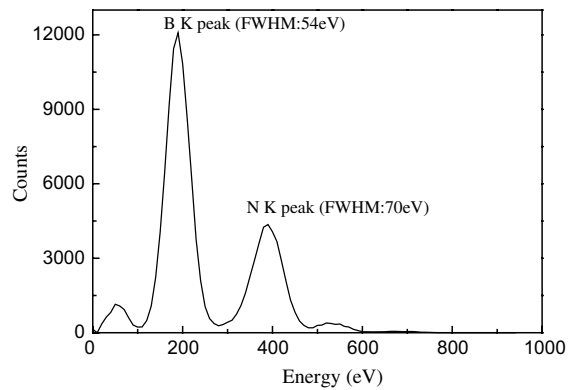


Fig. 5. Energy spectrum of boron nitride at 200 eV excitation collected by the 14-element array detector at the NSLS.

4. Conclusion

Our research resulted in the development of a new fabrication process for Si(Li) detectors with significantly improved detection efficiency for soft X-rays below 1 keV. Specifically, the dead-layer thickness was reduced by 40% and the charge collection efficiency at 277 eV (Carbon K_α) was increased by a factor of two. The synchrotron beam-line experiments represent the first experimental observation of incomplete charge collection effects from directly incident monochromatic tunable X-rays below 1 keV energy. These measurements provide a benchmark for detector crystals fabricated from further improved processes with reduced dead layer. Ultimately, this type of

information will form the basis of a future model to predict the low energy detector performance resulting from different fabrication processes. The 14-element detector system that was designed, installed and tested at the NSLS is a powerful tool to study the characteristic X-rays of the lightest elements.

Acknowledgment

This work was supported by Department of Commerce SBIR contract 50-DKNB-0-90091.

References

- [1] J.L. Campbell, J.A. Maxwell, T. Papp, G. White, X-ray Spectrom. 26 (1997) 223.
- [2] M.C. Lepy, J. Plagnard, P. Stemmler, G. Ban, L. Beck, P. Dhez, X-ray Spectrom. 26 (1977) 195.
- [3] F. Schloze, G. Ulm, Nucl. Instr. and Meth. A 339 (1994) 49.
- [4] B.G. Lowe, Nucl. Instr. and Meth. A 439 (2000) 247.
- [5] J.M. Jaklevic, F.S. Goulding, IEEE Trans. Nucl. Sci. 18 (1971) 187.
- [6] I. Uzonyi, Gy. Szabo, I. Borbely-Kiss, A.Z. Kiss, Nucl. Instr. and Meth. B 210 (2003) 147.
- [7] R.G. Musket, W. Bauer, J. Appl. Phys. 43 (1972) 4786.
- [8] The tail factor is defined as the ratio of the average background count in the energy range from E_1 to E_2 to the peak count in the $E_0 = 5.895$ keV ^{55}Fe K_{α} peak, where $E_1 = E_0 - 1.74$ keV + T , $E_2 = E_0 - T$ and $T = 1.58 \cdot \text{FWHM}(E_0)$.
- [9] The Peak-to-Background is defined from an ^{55}Fe spectrum as the ratio of the peak count at 5.895 keV to the average count in the background continuum between 900 eV and 1100 eV.
- [10] The TCL is defined as the ratio of the integral counts in the energy range from 300 eV to E_1 to the integral counts in the energy range from E_1 to E_2 centered on the $E_0 = 5.895$ keV ^{55}Fe K_{α} peak, where $E_1 = E_0 - T$, $E_2 = E_0 + T$ and $T = 2 \cdot \text{FWHM}(E_0)$.
- [11] H.R. Zullinger, D.W. Aitken, IEEE Trans. Nucl. Sci. 15 (1968) 466;
H.R. Zullinger, D.W. Aitken, IEEE Trans. Nucl. Sci. 16 (1969) 47.
- [12] J. Lacer, E.E. Haller, R.C. Cordi, IEEE Trans. Nucl. Sci. 24 (1977) 53.
- [13] H.L. Malm, IEEE Trans. Nucl. Sci. 22 (1975) 140.
- [14] W.L. Hansen, E.E. Haller, G.S. Hubbard, IEEE Trans. Nucl. Sci. 27 (1980) 247.
- [15] R.W. Fink, NBS Special Publication, 604 (1981) 5.
- [16] W. Pebara, Int. J. Appl. Radiat. Isot. 34 (1983) 519.
- [17] C.S. Rossington, J.T. Walton, J.M. Jaklevic, IEEE Trans. Nucl. Sci. 38 (1991) 239.
- [18] C.S. Rossington, R.D. Giaque, J.M. Jaklevic, IEEE Trans. Nucl. Sci. 39 (1992) 5570.